Supplementary Information:

Non-PGM electrocatalysts for PEM fuel cells: Effect of fluorination on the activity and the stability of a highly active NC_Ar+NH₃ catalyst

Gaixia Zhang,[a] Xiaohua Yang,[a] Marc Dubois,*[b] Michael Herraiz,[b] Régis Chenitz,[a] Michel Lefèvre,[a] Mohamed Cherif,[a] François Vidal,[a] Vassili P. Glibin,[c] Shuhui Sun*[a] and Jean-Pol Dodelet*[a]

a: INRS-Énergie, Matériaux et Télécommunications, 1650 Boulevard Lionel Boulet, Varennes, Québec, J3X 1S2, Canada

b: Université Clermont Auvergne, CNRS, SIGMA Clermont, Institut de Chimie de Clermont-Ferrand, F-6300 Clermont-Ferrand, France

c: Department of Chemical and Biochemical Engineering, University of Western Ontario, London, N6A 5B9, Canada
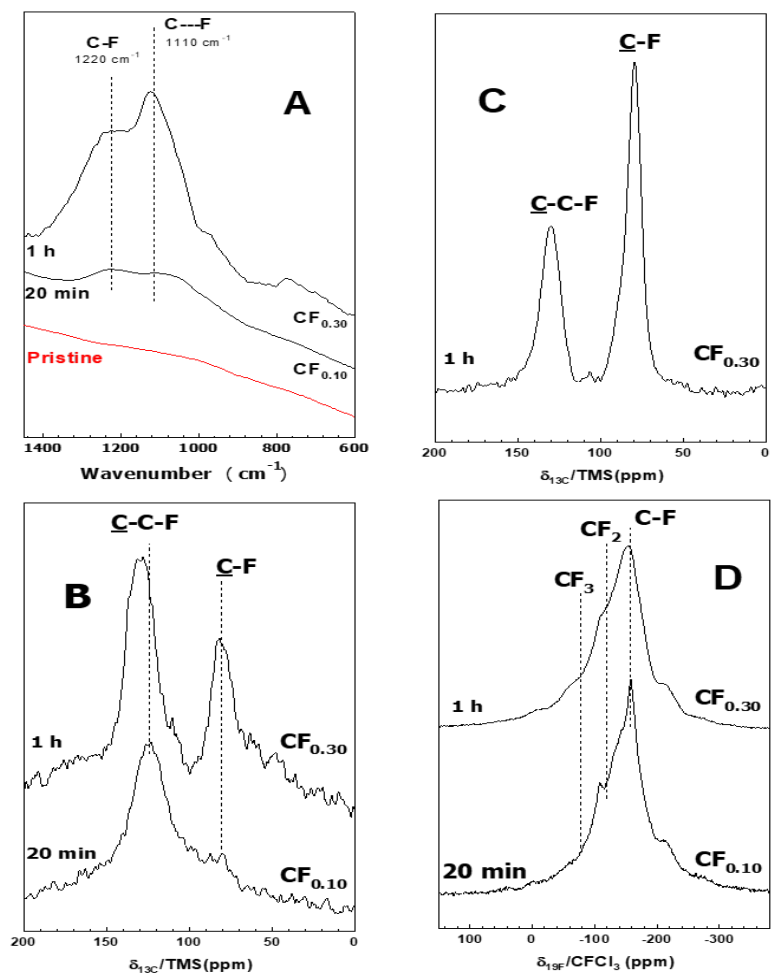
Figure S1: **N-doped Black Pearls** (A) FTIR (Attenuated Total Reflectance [ATR]) spectra of pristine BP-N, F20min-BP-N, F1h-BP-N, (B) ^{13}C Magic Angle Spinning [MAS], 10 kHz NMR spectra of F20min-BP-N, F1h-BP-N, (C) ^{19}F$\rightarrow$^{13}C Cross Polarization [CP] NMR spectra of the same samples, (D) ^{19}F MAS, 14 kHz NMR spectra of the same samples. Fluorination time (in min or h) is indicated in each panel as well as the C/F ratio given as CF$_X$.
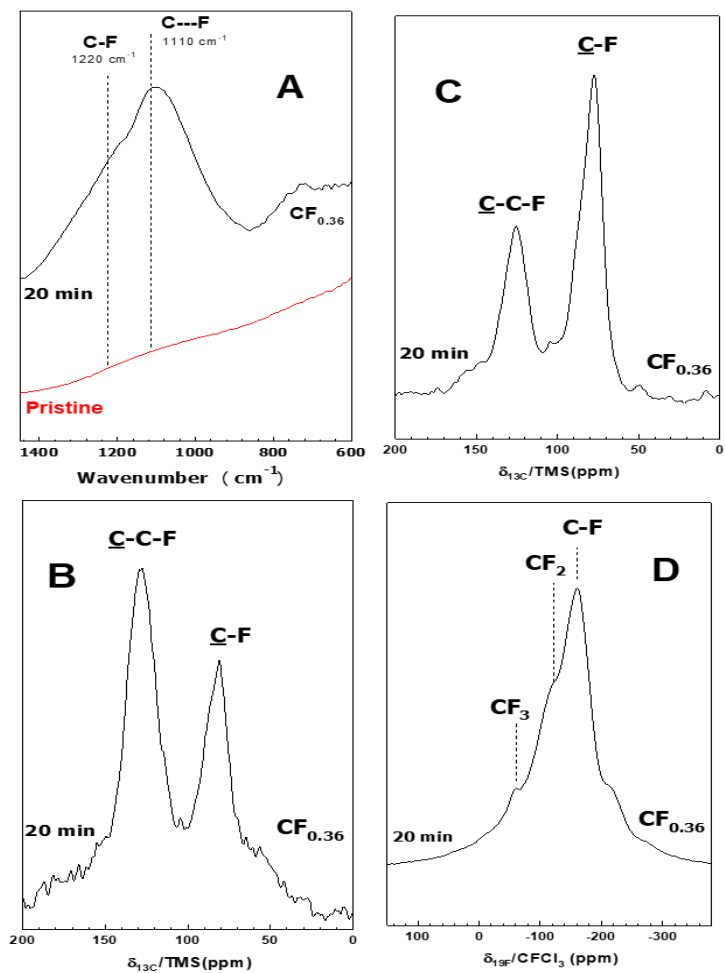
Figure S2: **Metal Organic Framework [MOF].** FTIR (Attenuated Total Reflectance [ATR]) spectra of pristine MOF, F20min-MOF, (B) ^{13}C Magic Angle Spinning [MAS], 10 kHz NMR spectra of F20min-MOF, (C) ^{19}F→^{13}C Cross Polarization [CP] NMR spectra of the same samples, (D) ^{19}F MAS, 14 kHz NMR spectra of the same samples. Fluorination time (in min) is indicated in each panel as well as the C/F ratio given as CF$_X$.
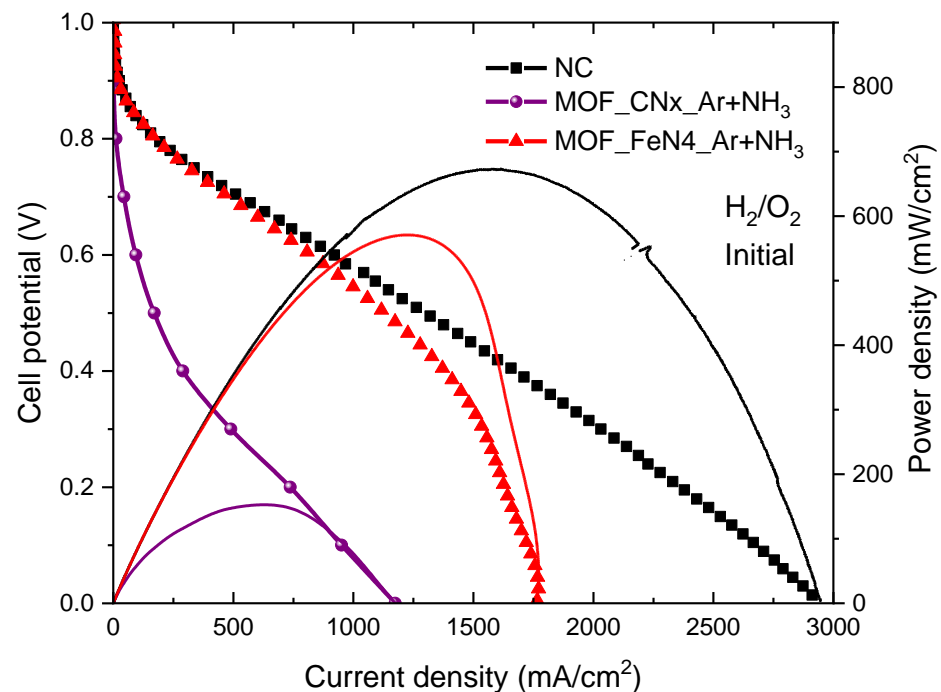
Figure S3 (**from Ref [33**] **in the main text**): Initial experimental polarization curve (left y axis) obtained at 80 °C in H_2/O_2 fuel cell for NC (black squares); Initial polarization curve (purple line) of MOF_CNx_Ar+NH$_3$ obtained, after extrapolation to 50 ppm Fe, for the current density of a catalyst made with ZIF-8 without any added iron; Calculation of the initial polarization curve (red line) obtained for MOF_FeNx_Ar+NH$_3$ by the subtraction of the purple line from the pink line. Corresponding power curves (right Y axis) for the two catalysts and for MOF_FeNx_AR+NH$_3$. The cathode catalyst loadings are about 4 mg cm^{-2}.
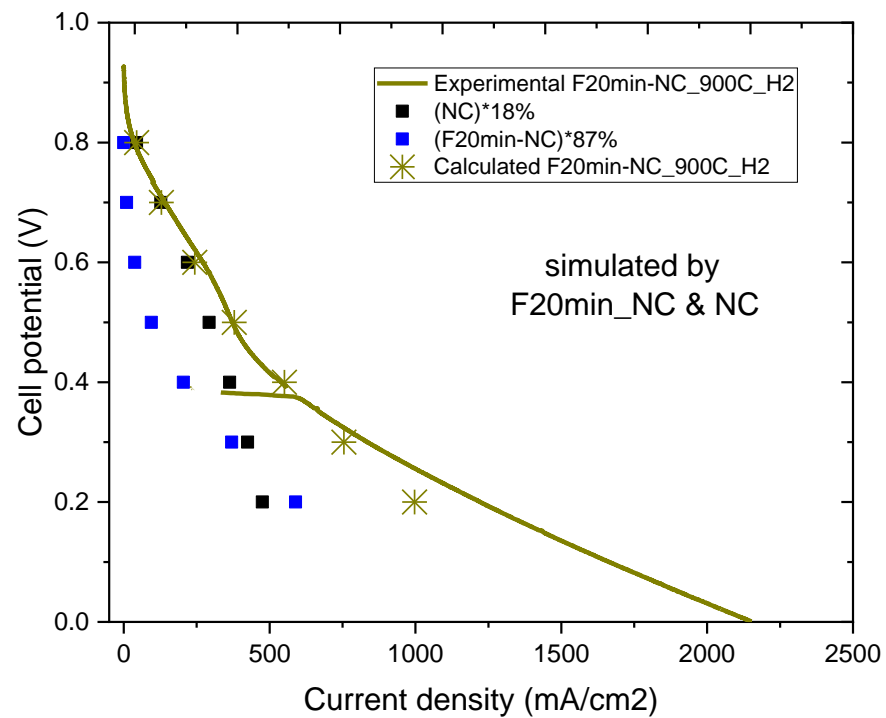
Figure S4: Experimental (dark yellow line) and simulated (at 0.8 to 0.2 V, dark yellow ✳) polarization curves for F20min-NC_900 ℃_H$_2$. The blue squares represent a 87% contribution to the total current density of the polarization curve for F20min-NC, while the black squares represent a 18% contribution to the total current density of the polarization curve for NC. Both 87% and 18% contributions to the respective current densities add to obtain the total simulated current density at 0.8 to 0.2V (✳). The rationalization of this simulation is given in the next page.

The yellow rectangle #1 represents a fraction of the surface area of un-fluorinated NC catalyst with all its active sites (FeNx, CNx, …) which are characterized in H_2/O_2 PEM fuel cell by the polarization curve given by the sequence of black squares in Figure 4A.

1 | NC

Catalytic sites: FeNx, CNx, …
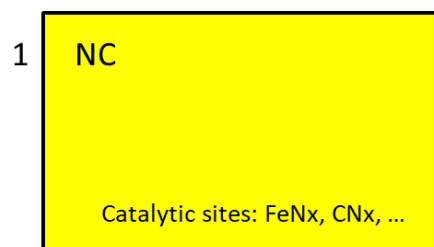
The blue rectangle #2 represents an identical fraction of the surface area of F20min-NC catalyst with all its FeNx sites poisoned by the 20 min fluorination of NC. The remaining active sites (CNx, …) are characterized in H_2/O_2 PEM fuel cell by the polarization curve given by the sequence of blue squares in Figure 4A.

2 | F20min-NC

Catalytic sites: CNx, …

The light blue rectangle #3 represents an identical fraction of the surface area of F20min-NC_900 ^{o}C_H$_2$ catalyst with FeNx sites still poisoned by the fluorination of NC during 20 min, except for the light yellow circles where poisoned FeNx sites have been reactivated by the heat-treatment at 900 ^{o}C in H$_2$.
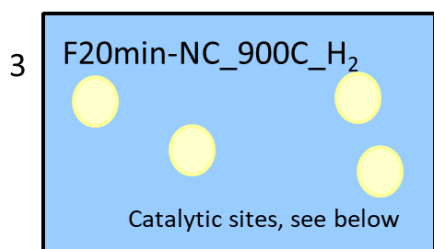
The micropores initially present in F20min-NC have been seriously etched by the heat-treatment at 900°C in H$_2$, enlarging them or transforming them into mesopores. Some of the catalytic sites originally present at the surface of (#1) NC or of (#2) F20min-NC have been etched away from the surface of the heat-treated catalyst, explaining why a lighter yellow or a lighter blue color is used to symbolize a lower content of catalytic sites in (#3) F20min-NC_900 ^{o}C_H$_2$ than in unpoisoned (#1) NC or (#2) fluorine poisoned F20min-NC.

3 | F20min-NC_900C_H$_2$

Catalytic sites, see below

Less CNx in [ ] than in [ ]

Less FeNx and CNx in ( ) than in [ ]

Therefore, the H_2/O_2 polarization curve of F20min-NC_900 ^{o}C_H$_2$ in Figure S4 represented by the symbol (✳) has been calculated at several potentials between 0.8 and 0.2V on the basis of a 87% contribution of the polarization curve given by the sequence of the blue squares in Figure 4A, and a 18% contribution of the polarization curve given by the sequence of the black squares in Figure 4A. The reduced contribution of the polarization curve in both cases illustrates the relative loss of catalytic sites that are resulting from H$_2$ etching of the catalyst surface.
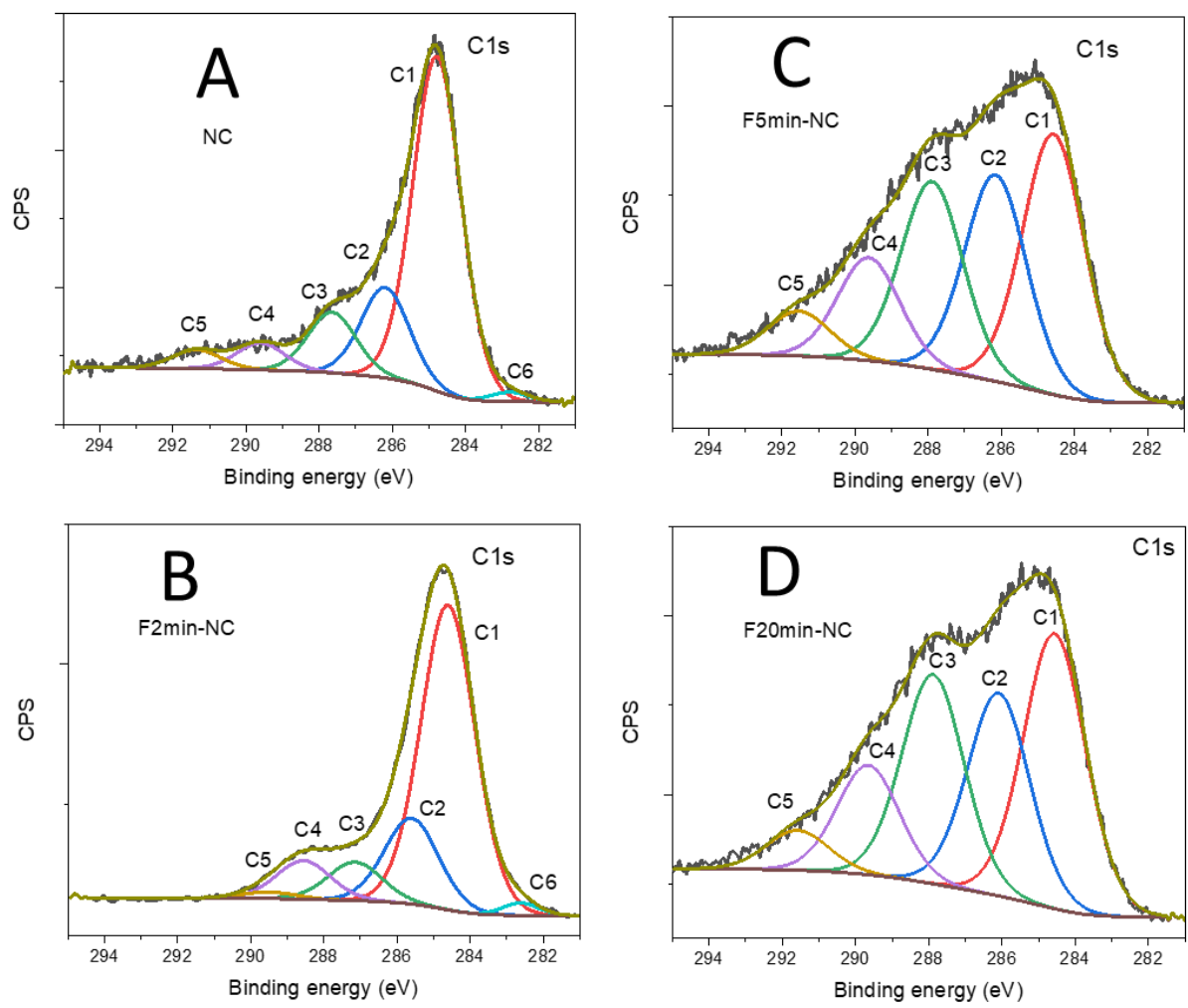
6

Figure S5: Deconvolution of the C1s XPS narrow spectra presented in Figure 5A for the NC catalyst after 0, 2, 5, and 20 min of fluorination.

Table S1

Relative and absolute carbon contents for the six deconvoluted peaks of the C1s XPS spectra recorded for unfluorinated and fluorinated NC catalysts before any heat-treatment.

Peak name	NC		F2min-NC		F5min-NC		F20min-NC	
	Relative content (%)	Absolute content (at%)	Relative content (%)	Absolute content (at%)	Relative content (%)	Absolute content (at%)	Relative content (%)	Absolute content (at%)
C1[a]	62.0	56.8	61.1	46.1	32.4	21.8	32.7	21.2
C2	16.8	15.4	18.7	14.1	25.7	17.3	24.3	15.7
C3	11.3	10.4	8.1	6.1	23.4	15.8	25.0	16.2
C4	5.0	4.6	8.2	6.2	12.9	8.7	13.1	8.5
C5	3.5	3.2	1.9	1.4	5.6	3.8	4.9	3.2
C6	1.4	1.3	2.0	1.5	0.0	0.0	0.0	0.0
C1s[b]	100.0	91.7	100.0	75.4	100.0	67.4	100.0	64.8

a: The absolute content for C1 in NC, for example, is obtained the following way: C1s absolute content for NC x C1 relative content for NC / 100 = 91.6 at% x 62.0% / 100% = 56.8 at%, etc…
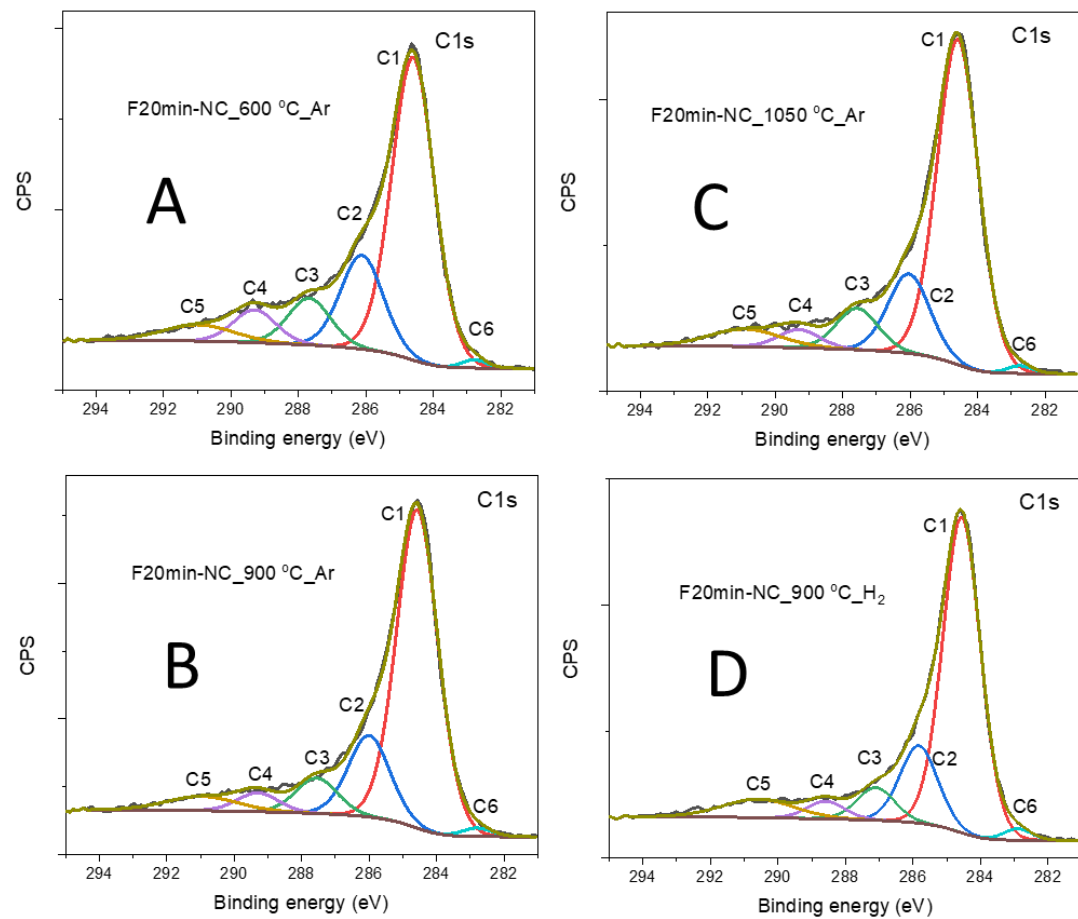b: The value of the C1s absolute content for NC and for the other catalysts is obtained from Table 1.

Figure S6: Deconvolution of the C1s XPS narrow spectra presented in Figure 5B for F20min-NC after various heat-treatments in Ar or H_2.

Table S2

Relative and absolute carbon contents for the six deconvoluted peaks of the C1s XPS spectra recorded for fluorinated F20min-NC catalysts before and after heat-treatments at various temperatures either under H_2 or Ar.

Peak name	F20min-NC		F20min-NC_900 °C_H₂		F20min-NC_600 °C_Ar		F20min-NC_900 °C_Ar		F20min-NC_1050 °C_Ar	
	Relative cont. (%)	Absolute cont. (at%)	Relative cont. (%)	Absolute cont. (at%)	Relative cont. (%)	Absolute cont. (at%)	Relative cont. (%)	Absolute cont. (at%)	Relative cont. (%)	Absolute cont. (at%)
C1[a]	32.7	21.2	64.8	61.5	59.5	51.4	65.7	60.6	65.1	61.2
C2	24.3	15.7	15.9	15.1	18.5	16.0	16.8	15.5	15.9	14.9
C3	25.0	16.2	6.7	6.4	9.2	7.9	7.3	6.7	8.3	7.8
C4	13.1	8.5	3.6	3.4	6.5	5.6	3.9	3.6	3.7	3.5
C5	4.9	3.2	7.3	6.9	5.4	4.7	5.1	4.7	6.1	5.7
C6	0.0	0.0	1.7	1.6	0.9	0.8	1.2	1.1	0.9	0.8
C1s[b]	100.0	64.8	100.0	94.9	100.0	86.4	100.0	92.2	100.0	93.9

a: The absolute content for C1 in F20min-NC, for example, is obtained the following way: C1s absolute content for F20min-NC x C1 relative content for F20min-NC / 100 = 64.7 at% x 32.7% / 100% = 21.2 at%, etc…

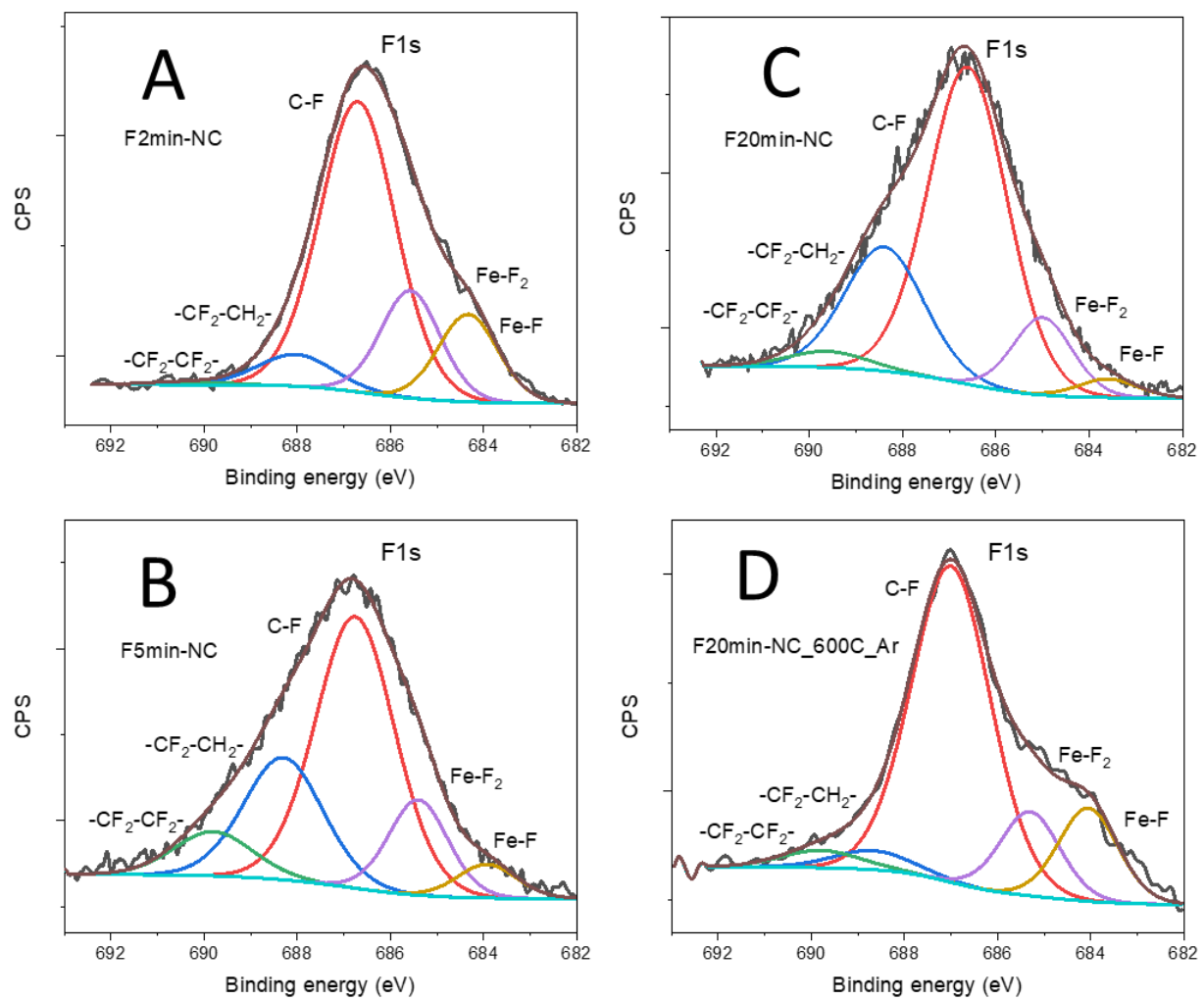b: The value of the C1s absolute content for F20min-NC and for the other catalysts is obtained from Tables 2 and 3.

Figure S7: Deconvolution of the F1s XPS narrow scan spectra presented in Figure 6A for Fxmin-NC, with x = 2, 5, and 20 min, and deconvolution of the F1s XPS narrow scan spectrum of F20min-NC after a heat-treatment at 600 ^{o}C in Ar.
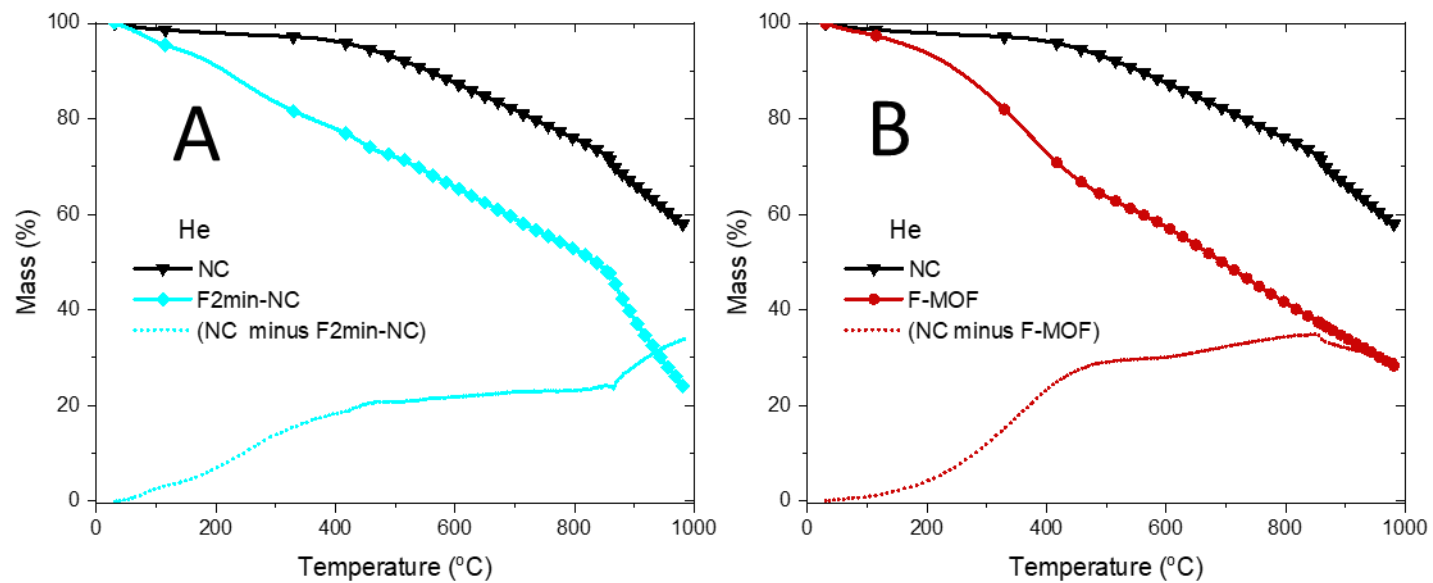
Figure S8: Thermal gravimetric analysis of: (A) NC, F2min-NC and of NC minus F2min-NC; (B) NC, F-MOF and NC minus F-MOF.
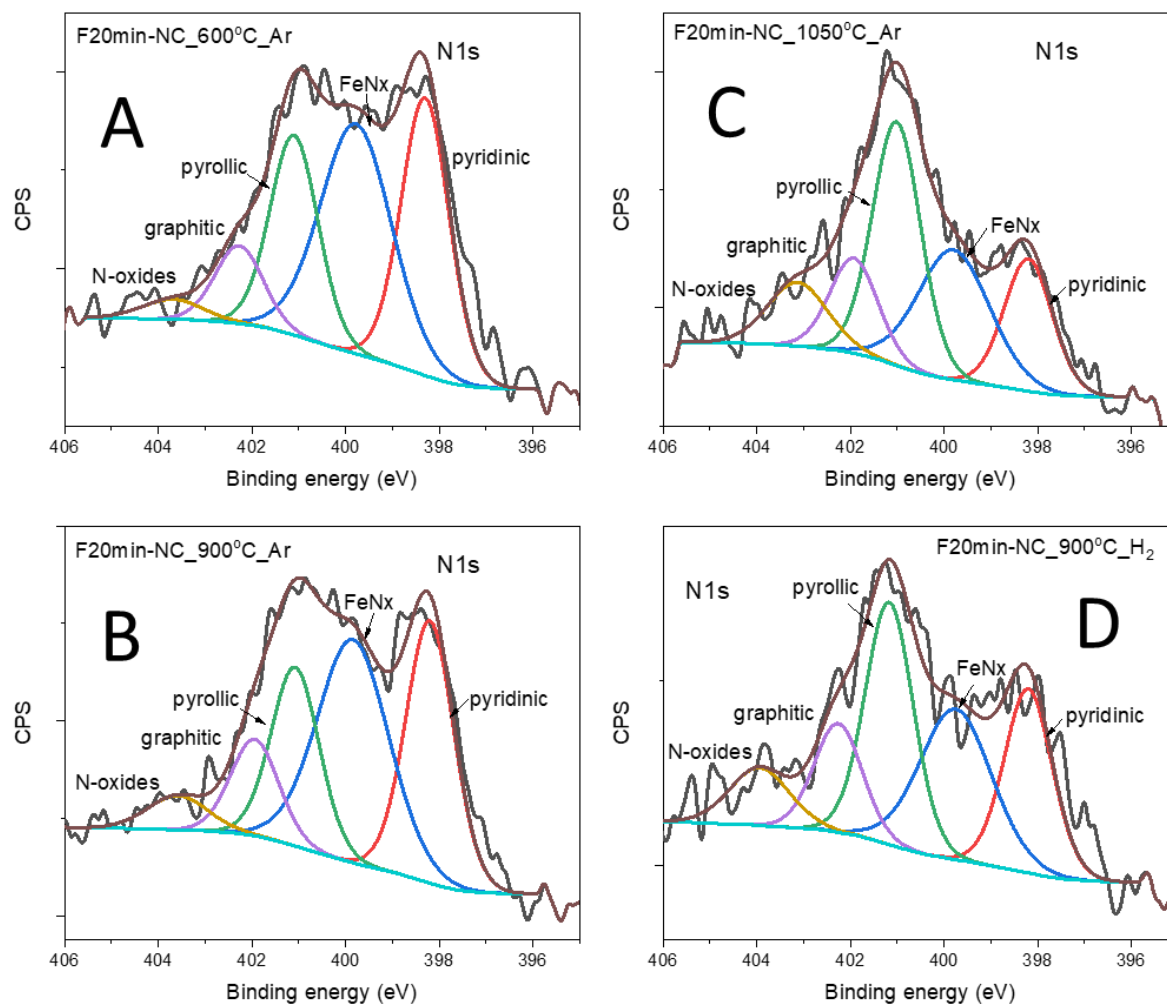
Figure S9: Deconvolution of the N1s XPS narrow spectra presented in Figure 6C for F20min-NC after various heat-treatments in Ar or H_2.

Table S3

Relative and absolute nitrogen contents for the six deconvoluted peaks of the N1s XPS spectra recorded for fluorinated F20min-NC catalysts before and after heat-treatments at various temperatures either under H_2 or Ar.

Peak name	F20min-NC		F20min-NC_900 °C_H_2		F20min-NC_600 °C_Ar		F20min-NC_900 °C_Ar		F20min-NC_1050 °C_Ar	
	Relative cont. (%)	Absolute cont. (at%)	Relative cont. (%)	Absolute cont. (at%)	Relative cont. (%)	Absolute cont. (at%)	Relative cont. (%)	Absolute cont. (at%)	Relative cont. (%)	Absolute cont. (at%)
Pyridinic[a]	13.7	0.4	22.1	0.3	30.1	1.1	28.7	0.9	17.8	0.3
Fm-FeN$_4$ with m= 0, 1, 2	42.5	1.4	27.0	0.4	37.2	1.3	36.5	1.1	26.1	0.5
Pyrrolic	19.1	0.6	29.1	0.4	21.6	0.7	19.6	0.6	32.7	0.6
Graphitic	15.2	0.5	13.1	0.2	8.4	0.3	10.6	0.3	12.8	0.2
Noxide	9.5	0.3	8.7	0.1	2.7	0.1	4.6	0.2	10.6	0.1
Iron nitride	0.0	0.0	0.0	0.0	0.0	0.0	0.0	0.0	0.0	0.0
N1s[b]	100.0	3.2	100.0	1.4	100.0	3.5	100.0	3.1	100.0	1.7

a: The absolute content for Npyridinic in F20min-NC, for example, is obtained the following way: N1s absolute content for F20min-NC x Npyridinic relative content for F20min-NC / 100 = 3.2 at% x 13.7 % / 100% = 0.4 at%, etc…
b: The value of the N1s absolute content for F20min-NC and for the other catalysts is obtained from Tables 2 and 3.
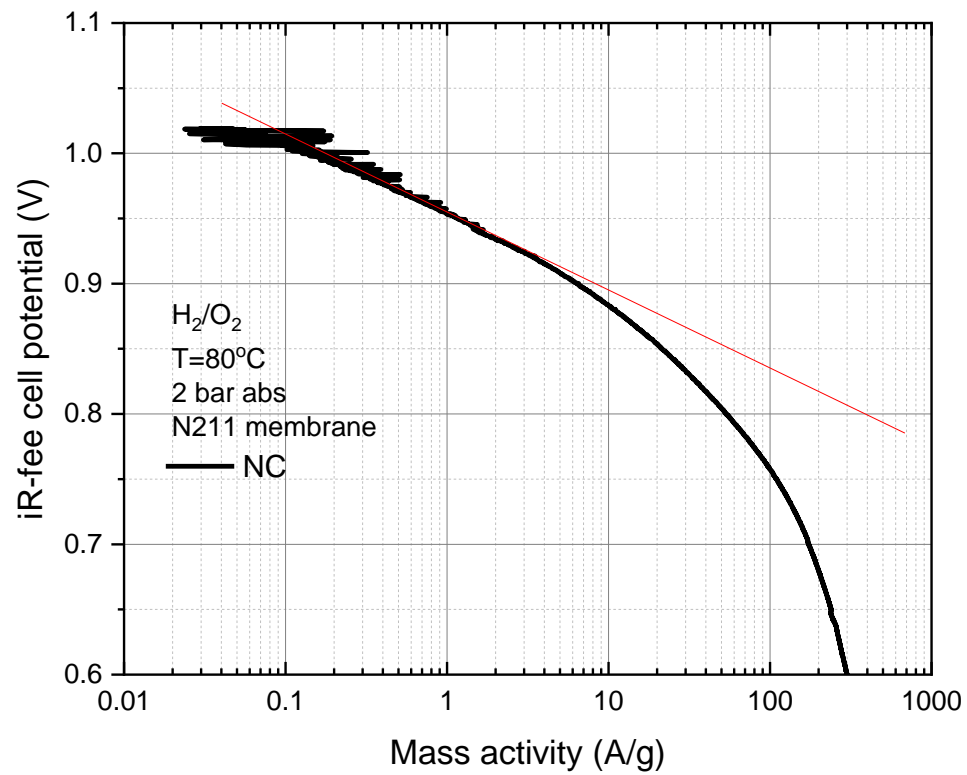
Figure S10: Initial polarization (black) curve at 80 °C in H_2/O_2 PEM fuel cell for NC and (red) Tafel line for iR-free cell potential vs log mass activity graph. Nafion / catalyst ratio: 1.25. Humidified gas absolute pressure: 2bar for both electrodes. Both gas flow rates: 0.3 sLpm. Membrane Nafion 211. The cathode catalyst loading is about 4 mg cm^{-2}.
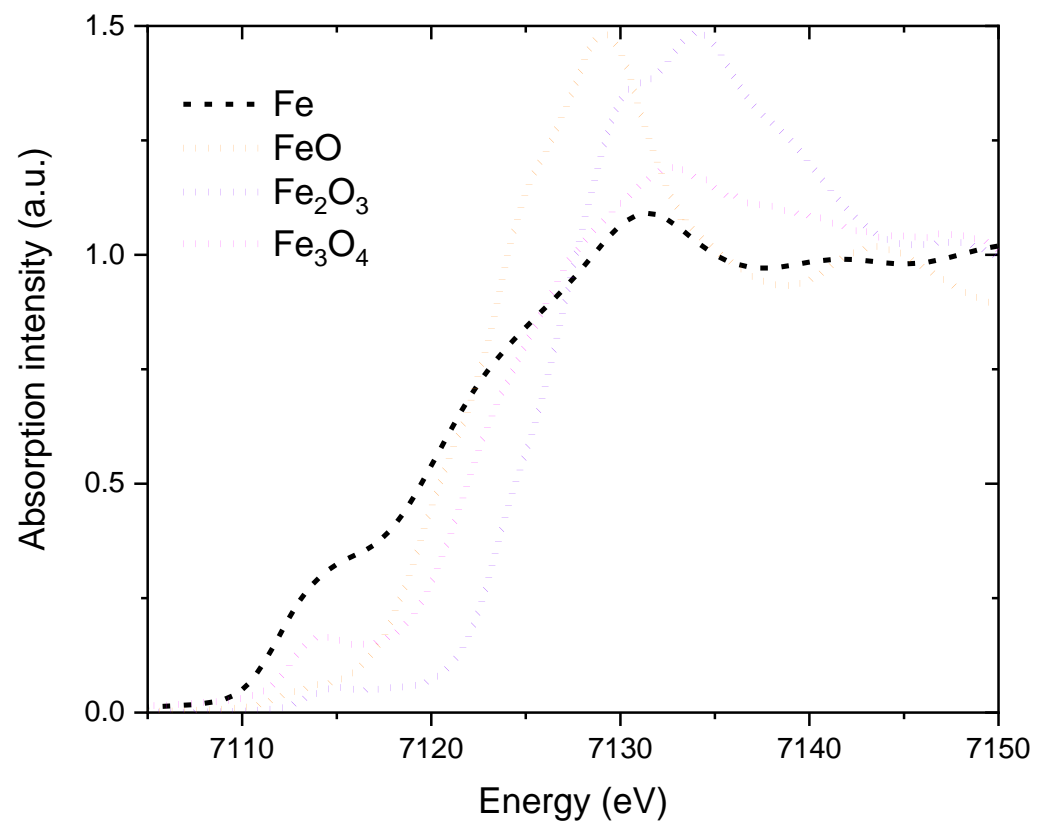
Figure S11: The normalized Fe K-edge XANES spectra of reference samples with Fe being either in (0), (II) and/or (III) oxidation states.
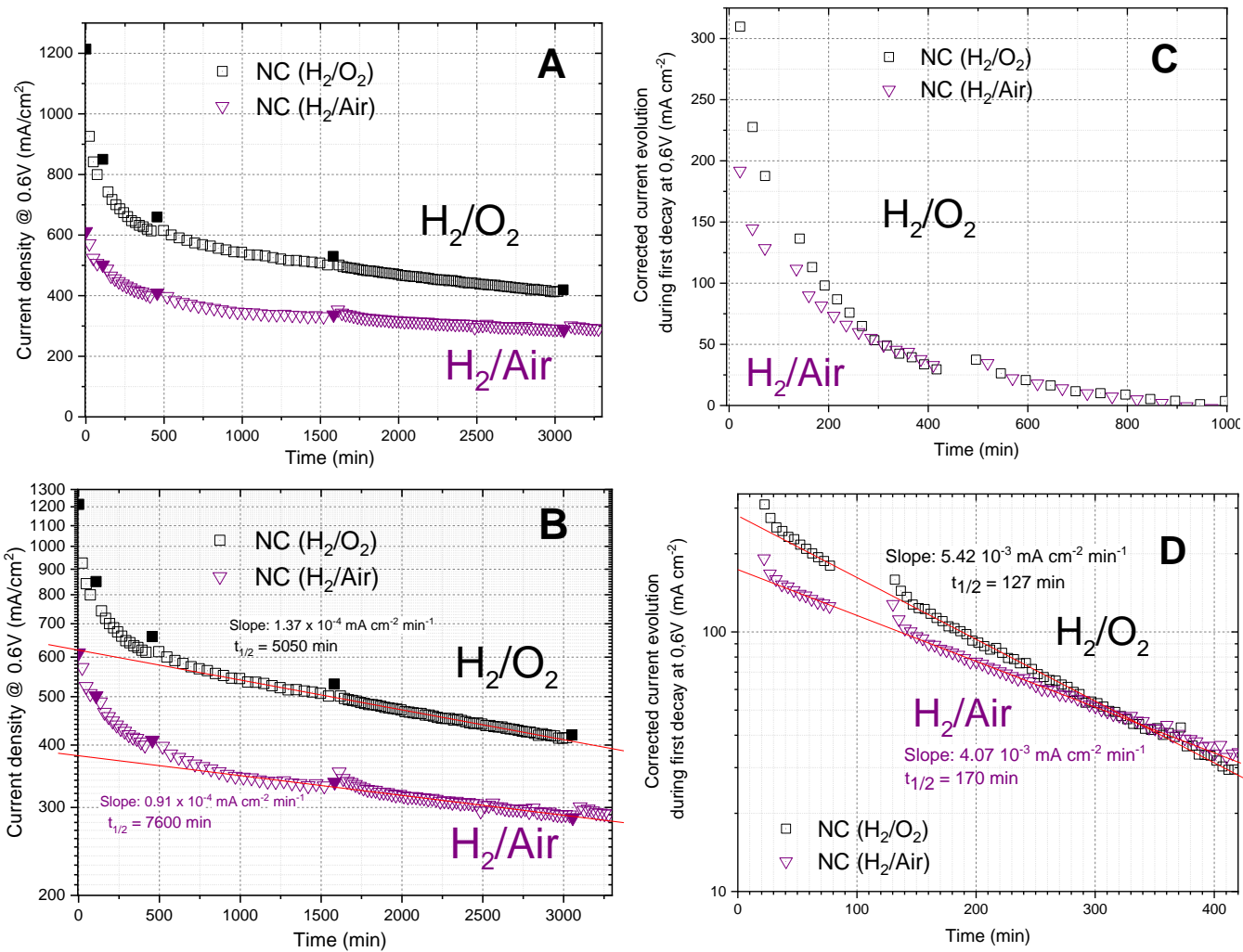
Figure S12: (A) Actual current density decay at 0.6 V in H_2/O_2 and in H_2/Air fuel cells; the cathode catalyst loadings are about 4 mg cm^{-2}.

(B) Same figure than for (A) except that the current density is now plotted on a Log_{10} scale.

The two red straight lines in (B) are used to obtain the adjustable parameters $j_{0,slow}$ and $t_{1/2,\ slow}$ for the H_2/O_2 and H_2/Air curves of the INRS model.

For instance, the current density at 0.6 V for the H_2/Air at t = 0 is 380 mA cm^{-2} and 283 mA cm^{-2} at t = 3250 min.

Slope = (Ln 380 – Ln 283) / 3250 = 0.91 x 10^{-4} mA cm^{-2} min^{-1}; and $t_{½,\ slow}$ = 0.693 / 0.91 x 10^{-4} = 7600 min.

(C) The differences between the experimental current densities in (B) and the respective red straight lines are reported for O_2 and for Air in (C).

They represent the actual fast exponential current decay in O_2 or in Air.

(D) Same figure than in (B) except that the current densities for the fast decay are now plotted on a Log_{10} scale.

The two red straight lines in (B) are used to obtain the adjustable parameters $j_{0,fast}$ and $t_{1/2,\ fast}$ for the H_2/O_2 and H_2/Air curves of the INRS model.

For H_2/O_2, $j_{0,fast}$ = 280 mA cm^{-2} and $j_{0,slow}$= 620 mA cm^{-2}; For H_2/Air, $j_{0,fast}$= 175 mA cm^{-2} and $j_{0,slow}$= 380 mA cm^{-2}.
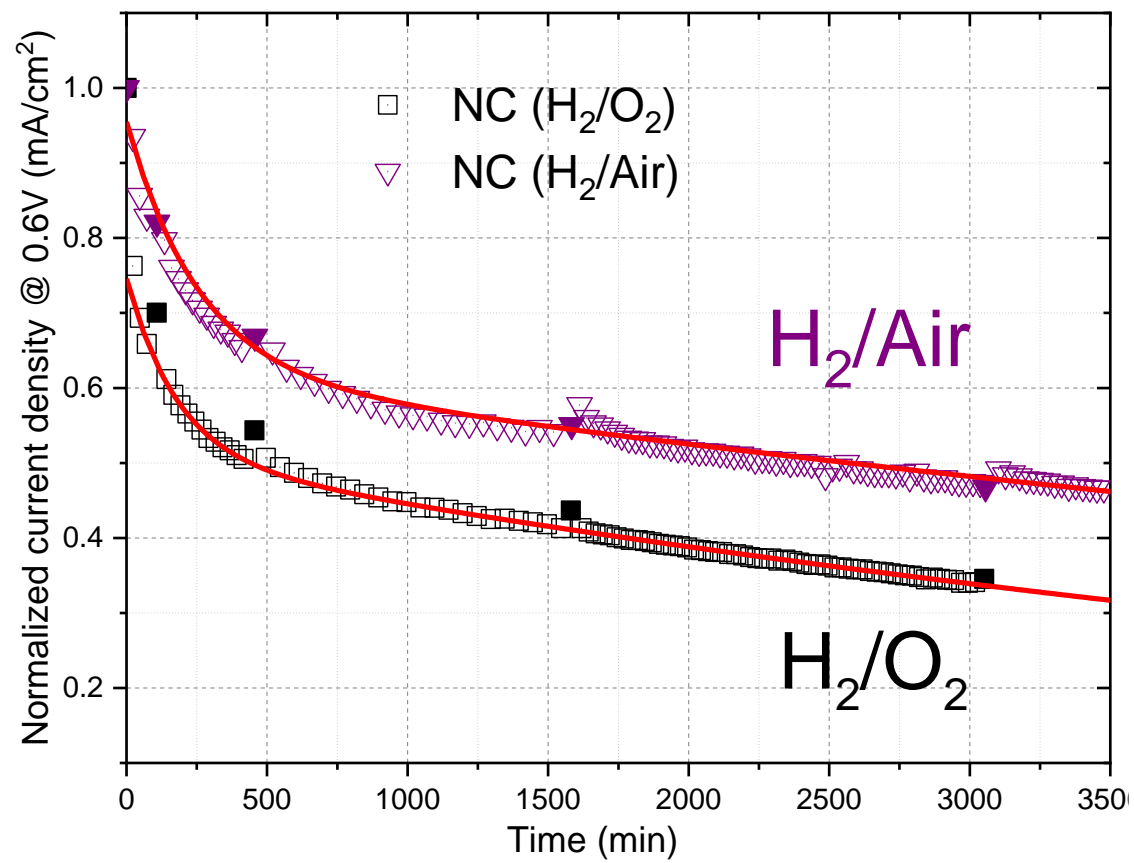
Figure S13: Normalized current density decay at 0.6V in H_2/O_2 and in H_2/Air fuel cells with superimposed curves obtained according to INRS model.
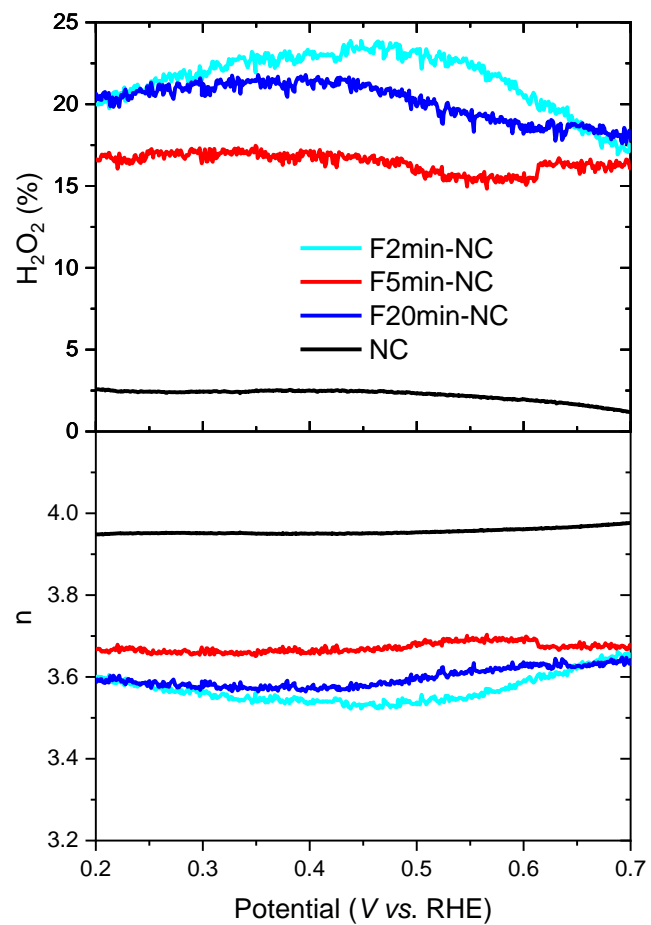
Figure S14: Room temperature RRDE determination at 1600 rpm of the value of n, the apparent number of electrons transferred during ORR, and %H$_2$O$_2$, as detected in O$_2$ saturated 0.1M HClO$_4$ for NC and for the three fluorinated Fxmin-NC. Each catalyst loading on the working electrode was 0.8 mg cm^{-2}.

Structural, chemical, and electrochemical comparison between NC and F20min-NC_900ºC_Ar

Given that no remaining F atoms are detected by XPS on F20min-NC_900ºC_Ar, why is this catalyst not performing at the same level than pristine NC? The following text will present: (i) the structural differences, (ii) the chemical differences, and (iii) the electrochemical differences between NC and F20min-NC_900ºC_Ar. The corresponding differences between NC and NC_900ºC_Ar will also be used for comparison.

(i)   Structural differences

Corrected Porosity ($m^2 g^{-1}$)	NC	→ F_2/N_2 → room temp	F20min-NC	→ 900ºC/Ar →	F20min-NC_900ºC_Ar
Micropores	947		435		796
Mesopores	155		230		91
	NC		→ 900ºC/Ar →		NC_900ºC_Ar
Micropores	947				949
Mesopores	155				176

One may argue that fluorination of NC will be particularly important at the edges of its micropores, blocking the access of FeN_4 catalytic sites of F20min-NC to H^+ and dissolved O_2 that were previously running freely through the un-fluorinated micropores of NC. Note that if some of the micropores of F20min-NC remain partially or fully open, fluorine will also poison their FeN_4 catalytic sites and the effect on the electrocatalytic performance of the fluorinated catalyst will be the same than for inaccessible un-poisoned FeN_4 sites.

One may also argue that the accumulation of a maximum of 26 at% of fluorine atoms in the mesopores may also increase the mesoporous surface area of F20min-NC.

When F20min-NC is heat-treated at 900ºC in Ar, all fluorine atoms present in the catalyst are expelled from the surface of its pores, but the total initial surface area of NC is not entirely recovered. It seems that part of the surface area of F20min-NC_900ºC_Ar collapsed during the fluorine removal process (thermal defluorination). In that case, one may argue that some FeN_4 sites that were initially accessible in NC become now secluded and become inaccessible in F20min-NC_900ºC_Ar. This has a negative effect on the final electrochemical performance of F20min-NC_900ºC_Ar compared with NC.

Nothing similar happens if NC is only heat-treated at 900°C in Ar. The high temperature heat-treatment is therefore not to blame for the loss of activity by structural reorganization. It is the defluorination which has an effect on the porosity of the final resulting catalyst: F20min-NC_900°C_Ar.

(ii)   Chemical differences

XPS quantification (at%)	NC	→ F$_2$/N$_2$ → room temp	F20min-NC	→ 900°C/Ar →	F20min-NC_900°C_Ar
C	91.6		64.7 [91.3]*		92.2
O	3.0		5.2 [7.3]		4.4
N	4.8		3.2 [4.5]		3.1
F	0.0		26.0		0.0
	NC	→ 900°C/Ar →			NC_900°C_Ar
C	91.6				91.0
O	3.0				4.7
N	4.8				4.2
F	0.0				0.0

Corrected chemical composition for the addition of 26.0 at% of fluorine to the catalyst

From the chemical point of view, the addition to the carbonaceous structure of NC of 26 at% of fluorine drastically modifies the atomic content of the other atoms (C, O, and N). However, if the chemical composition of the catalyst is corrected by the same factor: f = ((19 x 0.26) + 12) /12 = 1.41 than the one used to correct the porosity (see: Experimental section – Specific surface area), one obtains the corrected atomic contents for C, O, and N, reported between brackets in the Table above. In these conditions, one sees that, except for the oxygen content, which is not important for the catalytic activity, one obtains about the same chemical content for carbon and nitrogen in F20min-NC than in NC.

However, the nitrogen content decreases when F20min-NC is heat-treated at 900 °C. As fluorine and nitrogen atoms are removed during the thermal treatment, NF$_3$ gas would be evolved during the thermal defluorination in addition to primary gaseous products such as carbene (CF$_2$), and C$_2$F$_4$ (formed by the dimerization of CF$_2$). CF$_4$ and C$_2$F$_6$ may also be evolved [1]. This may have a negative effect on the catalytic activity since

N is part of the structure of the FeN_4 catalytic site. This negative effect may become important if it is conjugated with a decrease of the specific surface area of the micropores.

Heat-treating only NC (without proceeding through fluorination) also decreases the nitrogen content but much less than when NC is first fluorinated. In the latter case, it is probably the structural reorganization that is increasing the nitrogen loss since it has been shown in the main text that there was no loss of N as NF_3 upon fluorination of NC in the mild conditions used for this work.

(iii)   Electrochemical differences

Power ratio*1	NC	→ F_2/N_2 → room temp	F20min-NC	→ 900°C/Ar →	F20min-NC_900°C_Ar
%	100*2		15.7		68.7
	NC	→ 900°C/Ar →			NC_900°C_Ar
%	100				78.0

*1 Power ratio = Maximum power density for catalyst x / Maximum power density for NC
*2 100% identifies the maximum power density of NC with a value of 0.83 W cm^{-2}.

The electrochemical differences combine the structural and chemical differences.
Simply heating NC at 900°C in Ar decreases its maximum power in fuel cell by 100 – 78 = 22 % and this is mainly due to the loss of nitrogen upon heating since structurally NC and F20min-NC_900°C_Ar are very close. An additional loss of 78 – 68.7 = 9.3 % of the maximum power density in fuel cell is attributable to the structural reorganization of the catalyst after expulsion of the fluorine atoms.

[1] M. Herraiz, M. Dubois, N. Batisse, S. Hajjar-Garreau, and L. Simon "Large-scale synthesis of fluorinated graphene by rapid thermal exfoliation of highly fluorinated graphite" Dalton Transactions, **2018**, 47, 4596-4606.

ToF determination for NC at 0.8 and 0.85V vs RHE in H_2/O_2 PEM fuel cell at 80 ºC

As far as we know, there is no report in the literature of ToF values measured at 0.9 V in H_2/O_2 PEM fuel cell at 80 ºC for Fe/N/C electrocatalysts. Some ToF measurements were, however, reported in the literature for Fe/N/C catalysts at 0.8 V vs RHE. It is therefore of interest now to compare the ToF deduced for NC at 0.8 V with values already reported in the literature for similar Fe-based ORR catalysts.

By following Equations (3) to (7) in the main text, one obtains for NC:
J (at 0.8 V, 80 ºC, and 1 bar absolute back pressure) = 400 A g^{-1} x 0.37 g cm^{-3} x 0.575 = 85.1 A cm^{-3} or 85.1 Coulomb cm^{-3} sec^{-1}.
Here 400 A g^{-1} was read at 0.8 V on the red Tafel curve displayed in Figure S10. This Tafel curve represents the iR-free cell potential vs mass activity and has a slope of 59 mV/decade.

Since SD = 6.0 ± 0.7 x 10^{19} FeN_4 sites cm^{-3} in NC, this yields:
ToF at 0.8 V = 85.1 Coulomb cm^{-3} sec^{-1} / (6.0 ± 0.7 x 10^{19} FeN_4 sites cm^{-3} x 1.6 x 10^{-19} Coulomb $electron^{-1}$) = 8.7 ± 1.0 electrons $site^{-1}$ sec^{-1}.

Similarly, J (at 0.85 V, 80 ºC and 1 bar absolute back pressure) = 60 A g^{-1} x 0.37 g cm^{-3} x 0.575 = 12.8 A cm^{-3} or 12.8 Coulomb cm^{-3} $sec^{-1.}$
This yields: ToF at 0.85 V = 12.8 Coulomb cm^{-3} sec^{-1} / (6.0 ± 0.7 x 10^{19} FeN_4 sites cm^{-3} x 1.6 x 10^{-19} Coulomb $electron^{-1}$) = 1.33 ± 0.16 electrons $site^{-1}$ sec^{-1}.

Compared with Pt/C for which Gasteiger and collaborators [1] reported in H_2/O_2 PEM fuel cell at 0.8 V and at a pressure of 1.5 bar, a ToF of 25 electrons $site^{-1}$ sec^{-1} for 47 wt% Pt/C (from TKK), the ToF at 0.8 V of Pt/C is only (25/8.7 =) 2.9 times larger than that of NC at the same potential.
At 0.85 V, the ToF of Pt/C is (4.8/1.33 =) 3.6 times larger than that of NC at the same potential.
Furthermore, it is reported in the main text that at 0.9 V, the ToF of Pt/C is 5 times larger than that of NC measured in the same experimental conditions.
The difference in these ToF ratios is attributable to the differences in the Tafel slopes: 70 mV $decade^{-1}$ for Pt/C in Figure 4 of reference [1] but 59 mV $decade^{-1}$ for NC in Figure S10. The ToF ratios would remain constant at all potentials if both Tafel slopes were identical.

To come back to the comparison of the ToF deduced for NC at 0.8 V and 80 ºC in H_2/O_2 fuel cell with the values reported in the literature for Fe-based catalysts, ToF ranging from 0.023 to 1.7 electrons $site^{-1}$ sec^{-1} appeared in 2005 and after corrections to the conditions used for Pt/C, in the work of Gasteiger and collaborators [1]. After 2005, ToF measurements for Fe-based catalysts were not numerous. One finds for instance:
(i) ToF values between 0.31 and 0.40 electrons $site^{-1}$ sec^{-1} at 0.8 V and 80 ºC in H_2/O_2 fuel cells for different Fe loadings of a catalyst, made by

impregnation of iron acetate on a carbon black that was then heat-treated at high temperature in NH_3 [2]. Here SD was deduced from the total amount of Fe loaded on the carbon black; (ii) a ToF value of 11.4 electrons site^{-1} s^{-1} at 0.8 V and room temperature in H_2SO_4 solution at pH = 1, for another Fe-based catalyst also made by impregnation of iron acetate on carbon black, followed by a heat-treatment at high temperature in NH_3 [3]. Here SD was obtained from the concentration of the most ORR active FeN_4 Mössbauer doublet (D3) among all the Fe-species present in the catalyst.

It is only after 2014 that more elaborate ToF determination procedures appeared for Fe-based catalysts. The first one used CO chemisorption on FeN_4 sites. In order to do so, CO chemisorption had to be carried out at low temperature (-80 °C), since it was already reported that at room temperature, FeN_4 active sites for ORR are either not poisoned [4] or are only partially poisoned [5]. Using CO chemisorption combined with Mössbauer spectroscopy, Strasser and collaborators found ToF values between 0.5 and 1.5 electrons site^{-1} s^{-1} at 0.8 V, from measurements in $HClO_4$ solution at pH = 1 for catalysts made by impregnation of carbon black of iron chloride and polyaniline, either alone [6] or with several secondary N precursors, followed by a pyrolysis at high temperature in N_2 [7]. The use of gas like CO in the ToF determination enables to unravel the previously inaccessible relation between active site density, turn-over-frequency, and active site determination since CO will only chemisorb on accessible FeN_4 sites, while ^{57}Fe Mössbauer spectroscopy is able to detect all FeN_4 sites in the bulk of the catalysts. Additional information about the CO chemisorption technique and its application to Fe-based catalysts obtained from the pyrolysis of ball-milled iron acetate and ZIF-8 precursors yielded at 0.8 V in 0.1 M $HClO_4$ electrolyte ToF values between 0.18 and 0.45 electron site^{-1} sec^{-1} [8].

The second procedure proposed to quantify the FeN_4 active centers used nitrite (NO_2^-) adsorption on the FeN_4 sites, followed by reductive stripping [9]. In that case, a ToF of 1.6 ± 0.2 electrons site^{-1} sec^{-1} was measured at 0.8 V in an acetate buffer solution at pH5.2 for a Fe/N/C catalyst made with polydiaminonaphthalene and iron chloride (no carbon support) followed by a high temperature heat-treatment in N_2.

References:
[1]   H. A. Gasteiger, S. S. Kocha, B. Sompalli, F. T. Wagner, *Applied Catalysis B : Environmental* 2005, **56**, 9-35.
[2]   F. Jaouen, J. P. Dodelet, *Electrochim. Acta* 2007, **52**, 5975-5984.
[3]   U. Kramm, J. Herranz, N. Larouche, T. M. Arruda, M. Lefèvre, F. Jaouen, P. Bogdanoff, S. Fiechter, I. Abs-Wurmbach, S. Mukerjee, J. P. Dodelet, *Phys. Chem. Chem. Phys.* 2012, **14**, 11673-11688.
[4]   L. Birry, J. Zagal, J. P. Dodelet, *Electrochemistry Communications,* 2010, **12**, 628-631.
[5]   Q. Zhang, K. Mamtani, D. Jain, U. Ozkan, A. Asthagiri, *J. Phys. Chem. C,* 2016, **120**, 15173-15184.
[6]   N. R. Sahraie, U. Kramm, J. Steinberg, Y Zhang, A. Thomas, T. Reier, J. P. Paraknowitsch, P. Strasser, *Nature Communications*, 2015, **6**, 8618.
[7]   N. D. Leonard, S. Wagner, F. Luo, J. Steinberg, W. Ju, N. Weidler, H. Wang, U. Kramm, P. Strasser, *ACS Catal.* 2018, **8**, 1640-1647.
[8]   F. Luo, C. H. Choi, M. J. M. Primbs, W. Ju, S. Li, N. Leonard, A. Thomas, F. Jaouen, and P. Strasser, ACS Catal. 2019, 9, 4841.
[9]   D. Malko, A. Kucernak, T. Lopes, *Nature Communications*, 2016, **7**, 13285.

Logistic Model of Los Alamos: Limits of Applicability

It is important to mention that the Los Alamos model that fits well the current decay curve recorded at 0.84 V for their CM-PANI-Fe-C(Zn) catalyst, is also able to fit the current decay curve recorded at 0.8 V and at 80 °C in H_2/Air PEM fuel cell for the INRS NC catalyst. The experimental decay of the current density recorded at 0.8 V and over 125 h for NC is illustrated in reference [1], Figure 6B. The fit of the INRS curve with the Los Alamos model is reported by Yin and Zelenay in Figure 5 of reference [2] where it is labeled "Double exponential decay fit" for the INRS model to be compared with the "Logistic fit" for the Los Alamos model. In the same work,[2] Yin and Zelenay also recommend to only verify the models under low-current (high fuel cell voltage, i. e. > 0.7 V) conditions. It is shown below, however, that the Logistic model of Las Alamos is possibly able to fit the current decay curve of a catalyst like NC at 0.8 and 0.2V, but not at intermediate potentials.
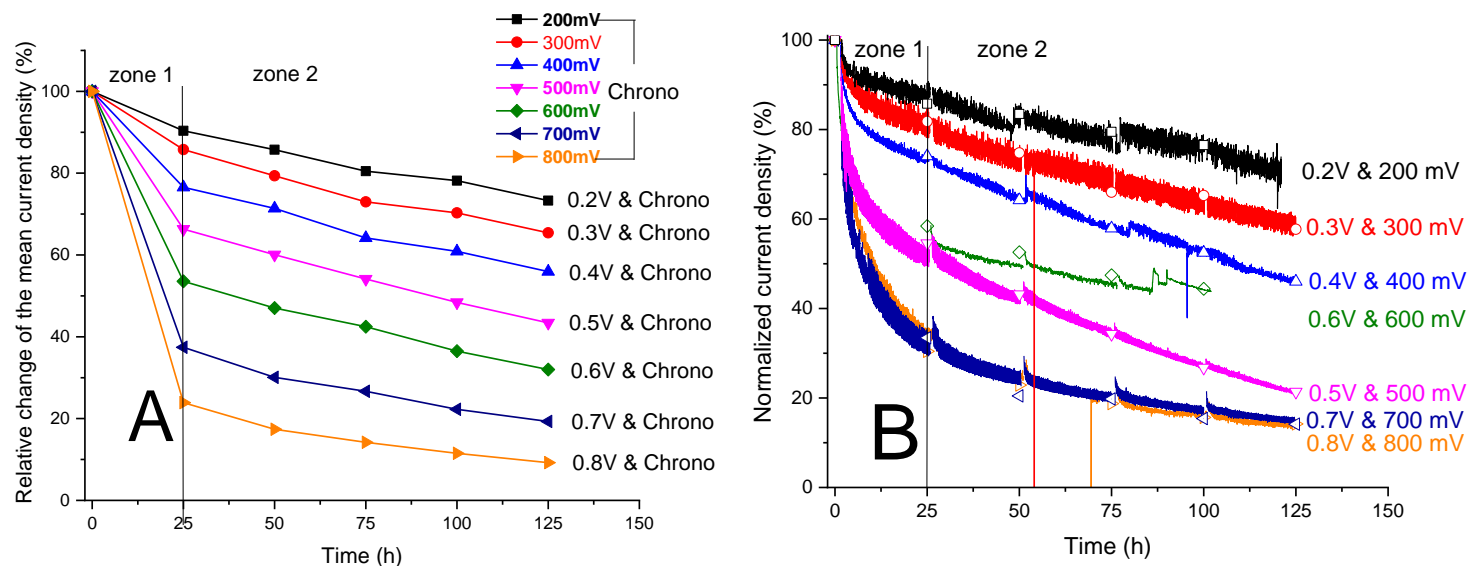

Fig. 6 of Ref. [1]: (A) Plot on the same graph of the **relative** changes in % of the **average** change in current density for the potentials between 0.8 and 0.2 V. The curve at each potential (V) is independent of the potential (from 200 to 800 mV) chosen to run the Chronoamperometry. (B) Plot on the same graph of the **relative** changes in % of the measured current density for the potentials between 0.8 and 0.2 V. Here V (the recording potential for each curve) and mV (the set potential for the Chronoamperometry) are the same.

To obtain Figure 6A of Ref. [1], a complete polarization curve was recorded every 25 h for each MEA held at a different potentials between 0.8 and 0.2 V. Each experimental point (at 25 h for instance) on a given curve (0.8 V for instance) is the mean value of the relative current density measured at 0.8 V for each of the seven MEAs used to obtain Fig. 6A and B of Ref. 1, independently of the potential at which each MEA was held (from 200 to 800 mV) during the Chronoamperometry between the recording of the polarization curves (see Ref [1] for details). Each curve of Figure 6A of Ref. [1] is therefore an average measurement over 7 MEAs of the relative current decay for NC.

Figure R1 presents the relative change of the current density for different values of t_0 calculated according to the Logistic current decay formula (displayed in Fig. R1), while Figure R2 is the combination of Figure 6A of Ref. [1] and Figure R1. One can see in Figure R2 that the Logistic model is possibly able to fit the experimental points of the relative current decay curves for 0.8 and 0.2 V. For the other potentials, the decay of the Logistic curve is too slow at the beginning of the current decay and too fast at the end. Figure R3 shows only the experimental decays that the Logistic curve is able to follow closely: at 0.8 V, $t_0 = 10$ h and at 0.2 V, $t_0 = 300$ h.
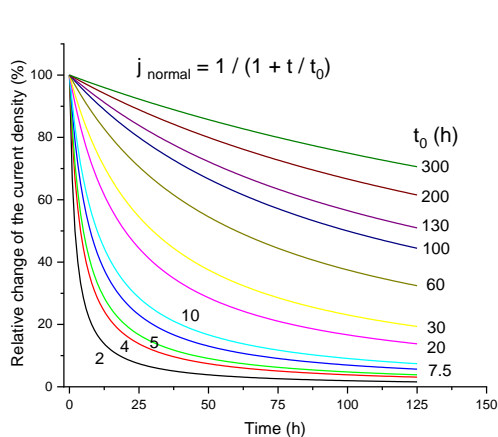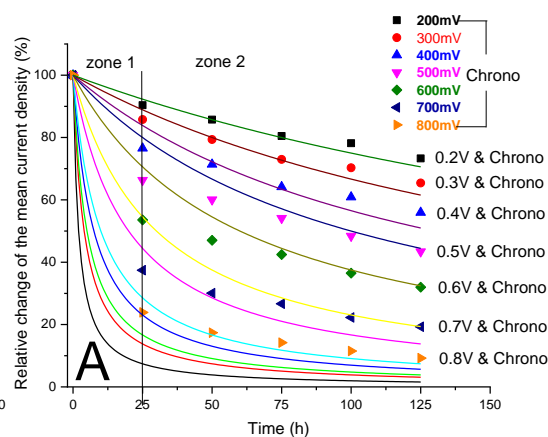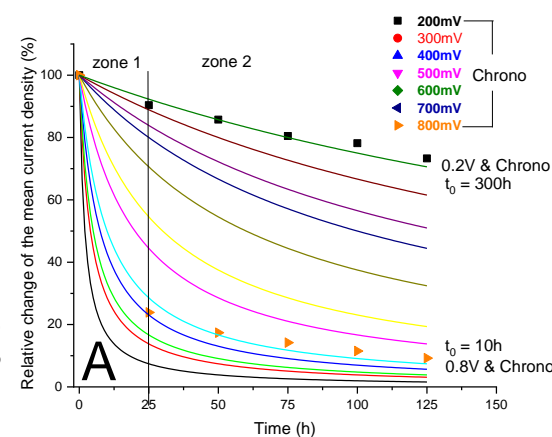

Figure R1

Figure R2

Figure R3

References :
[1]   R. Chenitz, U. Kramm, M. Lefèvre, V. Glibin, G. Zhang, S. Sun and J. P. Dodelet, Energy Environ. Sci. 2018, **11**, 365-382.
[2]   X. Yin and P. Zelenay, ECS Transactions, 2018, 85 (13) 1239-1250.